

Structural Brain Network Augmentation via Kirchhoff's Laws

Iman Aganj¹, Gautam Prasad², Priti Srinivasan¹, Anastasia Yendiki¹, Paul M. Thompson^{2,3}, and Bruce Fischl^{1,4}

¹Martinos Center for Biomedical Imaging, Radiology Department, Massachusetts General Hospital, Harvard Medical School, Boston, MA, United States, ²Imaging Genetics Center, Institute for Neuroimaging and Informatics, University of Southern California, Los Angeles, CA, United States, ³Depts. of Neurology, Psychiatry, Engineering, Radiology and Ophthalmology, University of Southern California, Los Angeles, CA, United States, ⁴Computer Science and Artificial Intelligence Laboratory, Massachusetts Institute of Technology, Cambridge, MA, United States

TARGET AUDIENCE: Researchers studying structural brain connectivity using diffusion MRI tractography.

PURPOSE: Diffusion-weighted (DW) MRI tractography is a noninvasive tool that can quantify structural connectivity between brain regions. Networks representing connectivity among different brain areas, known as the *connectome*¹, can be used to study how brain architecture is influenced by genetic factors, and changes during development and with disease. Standard approaches to compute structural connectivity often define the connection strength between two brain regions based on the tractography streamlines between them. Such a direct fiber bundle is expected to be the major signal carrier, however, multi-synaptic neural pathways – connecting the two areas through other regions – may also provide connectivity.² Here we propose to exploit the mathematical convenience provided by Kirchhoff's circuit laws to account for indirect pathways. We evaluate our model by assessing how well the network-derived measures can distinguish Alzheimer's disease patients from healthy controls.

METHODS: We model the multiple pathways connecting two regions starting with two simple cases. Figure 1 (left) shows two different fiber bundles connecting regions A and B, with x and y being the two connectivity measures corresponding to the two bundles, as returned by the tractography method. In this case, since more neural connections are expected to increase the connectivity, we consider the total connectivity between the two regions to be the sum of the individual bundle connectivity strengths, as $C_{A,B} := x + y$. The second basic case of our model, depicted in Fig. 1 (right), concerns the indirect connections between two regions, C and E, when the tractography has not returned any direct connections between them, but a third region, D, indirectly connects the two through fiber bundles connecting D to C and E, with strengths z and w , respectively. In this case, we consider the total connectivity between the two regions to be positive, but smaller than each of z and w . This is because the total connectivity is assumed to be bottlenecked by the weakest connectivity along the way (in colloquial terms: a chain is only as strong as its weakest link). To accommodate this, we model the connectivity in such a configuration as the inverse of the sum of inverses (i.e., twice the harmonic mean) of the individual connectivity strengths, as $\frac{1}{C_{C,E}} := \frac{1}{z} + \frac{1}{w}$.

Some more complex connectivity networks can be modularized, where each module is one of the two prior cases, making it possible to compute the total connectivity between every pair of regions recursively. However, this is not generally possible for an arbitrary network; so we exploit the similarity of the basic cases of our model to those of the electrical circuits made solely of resistors, and calculate the total connectivity between pairs of regions similarly to well-developed techniques in electronics. By analogizing individual connectivity of each fiber bundle to the electrical conductance (inverse of resistance) of a resistor, the two basic cases of our model are seen to be similar to parallel and series circuits. Therefore we use the Kirchhoff's circuit laws³ to compute the total connectivity between pairs of brain regions, using standard graph Laplacian methods.

RESULTS: We validate the proposed model on a dataset of 200 subjects from the second phase of the Alzheimer's Disease Neuroimaging Initiative (ADNI-2), composed of 50 cognitively normal controls, 74 early- and 39 late-stage mild cognitively impaired subjects (eMCI, IMCI), and 37 Alzheimer's disease (AD) patients. A 3T GE Medical Systems scanner at 14 acquisition sites in North America was used to capture whole-head MR images. The images included T1-weighted IR-FSPGR (spoiled gradient echo) anatomical scans (256x256 matrix; voxel size = 1.2x1.0x1.0 mm³; T1 = 400 ms; TE = 2.85 ms; flip angle = 11°). 46 DW images (35 cm field of view, 128x128 acquired matrix, reconstructed to a 256x256 matrix; voxel size: 2.7x2.7x2.7 mm³; scan time = 9 min) were collected that included 5 b₀ T2-weighted images (with no diffusion sensitization) and 41 DW images with b = 1000 s/mm². The DW-MRI volumes were corrected for head motion and eddy current distortions using FSL⁴. The brain was automatically located in the images using the Brain Extraction Tool⁵, and the extra-cerebral tissue was removed from the T1 images using ROBEX⁶, along with FreeSurfer⁷ and manual editing. These anatomical scans were corrected for intensity inhomogeneity using N3⁸ and aligned to the Colin27 brain template⁹ using FSL FLIRT⁴. The T1 images were registered to the b₀ images first linearly and then using inverse-consistent mutual information¹⁰. They were then segmented into 68 cortical regions (34 in each hemisphere) automatically computed using FreeSurfer⁷, and the label images were dilated with an isotropic box kernel of 5x5x5 voxels to ensure the labels overlapped with the white matter for the connectivity analysis. The orientation distribution functions in constant solid angle¹¹ were constructed and given to the Hough-transform global probabilistic tractography¹², which resulted in close to 10,000 fibers per subject.

Next, we made the 68x68 raw connectivity matrices without applying any normalization based on the fiber count or seed region size, and also computed the proposed augmented network matrices. The matrices were thresholded with 10 different values, and 35 network measures² were computed using the Brain Connectivity Toolbox¹ from all the matrices. For each pair of groups chosen from {Normal, eMCI, IMCI, AD}, we trained a Support Vector Machine (SVM) using the 35 network features and assessed the classification accuracy of each kind of network (raw or augmented) via a leave-one-out cross-validation. For each feature, kind of network, and pair of groups, we chose the threshold with the best *t*-test performance in distinguishing the groups. A third SVM was also trained using both sets of features from the raw and augmented networks (70 features). Figure 2 illustrates the classification error for each of the three methods.

DISCUSSION: As Fig. 2 demonstrates, combining the raw and augmented matrices resulted in the best classification among the Normal, eMCI, and IMCI groups. When classifying AD versus Normal and IMCI, the proposed (combined) network augmentation did not change the results. This may be due to the fact that the direct connections in AD patients show enough difference for the classification to work well without considering multi-synaptic connections. The eMCI/AD classification is the only one where the proposed combined method degrades the classification by overfitting. Since in only 1 out of 6 comparisons the combination of raw and augmented networks results in higher error compared to using each network alone, we deduce that the two networks contain complementary information.

CONCLUSION: We used techniques developed for processing the electrical circuit models to account for multi-synaptic connections in the brain and computed an augmented structural brain network from the DW-MRI data. We showed the combination of the features derived from raw and augmented networks to better classify the Normal, eMCI, and IMCI groups, not change the Normal/AD and IMCI/AD classifications, and worsen the eMCI/AD classification. The circuit model was only used for its computational convenience; we do not suggest that the resistive circuit is an appropriate model for the brain's biological wiring. Future research includes further validation of the proposed method with regard to the degree of consistency between structural and functional brain networks, and investigating the effect of finding and keeping only relevant network features in the analysis.

REFERENCES: 1) Rubinov & Sporns, *NeuroImage*'10. 2) Prasad *et al*, *ISBI*'13. 3) Bakshi & Bakshi, 2008. 4) Jenkinson *et al*, *NeuroImage*'12. 5) Smith, *HBM*'17. 6) Iglesias *et al*, *TMI*'11. 7) Fischl, *NeuroImage*'12. 8) Sled *et al*, *TMI*'98. 9) Holmes *et al*, *JCAT*'98. 10) Leow *et al*, *TMI*'07. 11) Aganj *et al*, *MRM*'10. 12) Aganj *et al*, *MedIA*'11.

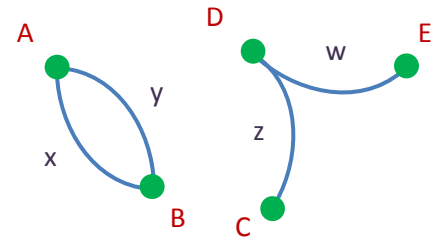


Fig. 1. Two basic cases of multiple connections.

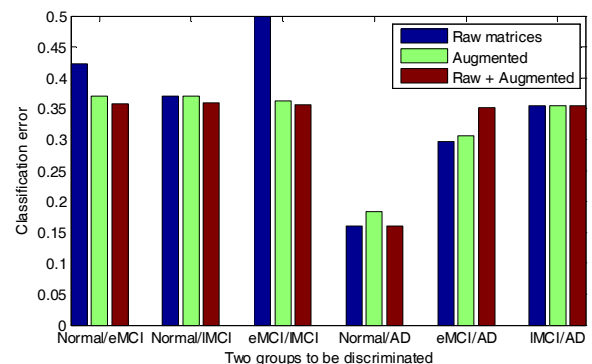


Fig. 2. Classification error using different methods.